FMC3-3
Invited

Simulation of micro-mirror array plates with Blender

Naoya Koizumi

koizumi.naoya@uec.ac.jp
[1]The University of Electro-Communications, 1-5-1 Chofugaoka, Chofu, Tokyo, Japan
Keywords: Mid-air image, micro-mirror array plates, ray tracing.

ABSTRACT

The characteristics of micro-mirror array plates (MMAPs) can be reproduced by computer graphics-based simulation using ray tracing with appropriate modeling. To simulate MMAPs, we investigated appropriate modeling methods and evaluated the validity of the simulation by comparing the characteristics of the rendered images with the actual images.

1 INTRODUCTION

Micro-mirror array plates (MMAPs) are a type of optical element that can generate mid-air images. When MMAPs are installed in combination with light sources, they can display mid-air images in real space. MMAPs have several characteristics. The light from the source is formed as a mid-air image at a plane-symmetrical position with respect to the MMAPs. However, undesired images are also produced that tend to disturb the observer. In addition, the viewing range in which the mid-air image can be observed is limited; this range changes depending on the design parameters of the optical system, such as the distance between the light source and MMAPs. Furthermore, the luminance of the mid-air image generated by the MMAPs is reduced to less than half that of the light source. For these reasons, it is difficult for designers without sufficient knowledge of optics to design a mid-air imaging system. Fig. 1 shows the structure of the MMAPs.

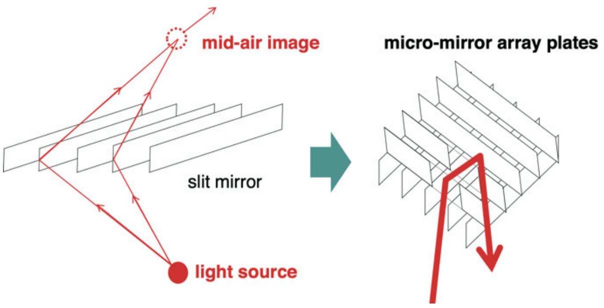

Fig. 1 Structure of micro-mirror arrays plates

To verify our simulation accuracy, we collected the characteristics of an actual system using MMAPs and a camera. This included the shape, position, and luminance of the mid-air image, and undesired images, and comprised our ground truth data. Based on these data, we found that the appearance of the mid-air image and characteristics of the MMAPs could be reproduced by a CG-based simulation using ray tracing with appropriate modeling parameters of the MMAPs. The CG mid-air image rendered in this simulation is shown in Fig. 2.

Fig. 2 Actual photo and simulation image

2 Related work

Several methods are available for forming mid-air images, such as a Fresnel lens [1], concave mirror [2], dihedral corner reflector array (DCRA) [3], ASKA3D plate [4], roof mirror array (RMA) [5], and aerial imaging by retro-reflection (AIRR) [6]. In this study, we chose to simulate ASKA3D, which is already commercially available and easy to purchase, and will be referred to in the rest of this paper simply as MMAPs.

3 Modeling

We modeled the MMAPs using the Blender software toolkit by referring to actual MMAPs [7]. The modeled MMAPs are optical imaging devices manufactured by Asukanet. The MMAPs are composed of two orthogonal overlapping slit mirror arrays consisting of 1,380 mirror-deposited micromirrors on both sides of a 0.5 mm thick and 1.5 mm high soda-lime glass plate. The total number of mirror arrays is 1,380 × 2 = 2,760, with the spacing between each mirror being 0.5 mm. When modeling this mirror array, we assumed that the method of modeling the glass was not important because the mid-air image obtained by MMAPs was formed by the reflection from a mirror, while the glass was made of a material with very high transparency. Hence, after arranging the mirror objects, we placed a glass object so that it just covered all the mirrors. The material of the glass was transparent with microfacets, and the index of refraction (IOR) was set to 1.52, which is the IOR of actual soda-lime glass. The reflectivity of the mirror material was set to 87% based on the luminance evaluation. All the modeling was performed assuming that the unit distance in Blender was 1 cm in real space.

4 Result

We evaluated the applicability of our simulation method for actual optical system design by comparing the simulation results to existing mid-air imaging optical systems. The evaluation results showed the characteristics of MMAPs, such as plane symmetry and undesired images. As shown in Fig. 3, a limited viewing range and luminance decay were also simulated using our modeling method.

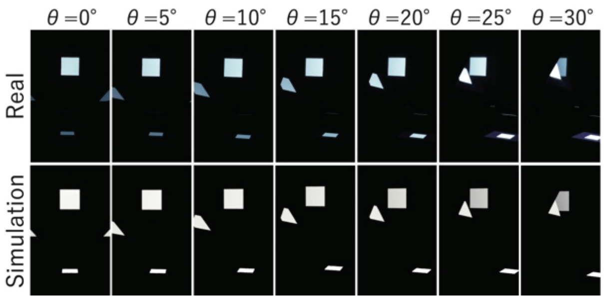

Fig. 3 Evaluation

5 Combination with computer vision

It is possible to implement automatic stray light detection, in which the rendered image is processed by computer vision [9]. We set the range for the camera position being rendered to the range where the mid-air image can be seen without disappearing, and the stray light is detected using the difference in the image appearance depending on the number of light reflections within the range.

To detect stray light, the simulator used the relationship between the number of reflections of the MMAPs and the number of bounces in the rendering process. The direction of light incident on the MMAPs is determined by the number of reflections at each layer. If each layer has an odd number of reflections, the light is properly retransmitted and can be observed as a mid-air image. However, when the number of reflections in each layer is even, it is observed as stray light. The number of bounces is the number of times a ray of light is branched by reflection or refraction when tracking a ray of light from the viewpoint of the light source. In other words, when the number of bounces is zero, only direct light can be observed.

In this study, we simulated the optical structure of EnchanTable [11], an optical system for displaying a mid-air image on a table, as shown in Fig. 4. To detect only stray light, the mid-air image is removed by changing the number of bounces in the rendering process. The transmitted light without any reflection is observed with a one bounce, as shown in Fig. 5. Stray light can be observed on the reflective surface with one layer of MMAPs and three bounces on the glass, while the mid-air image can be observed with four bounces by adding another layer.

Next, we describe the image processing approach for stray-light detection. First, the images of the mid-air image, stray light, and transmitted light were binarized. Subsequently, the white pixels were counted. The amount of stray light was calculated by subtracting the number of pixels for the mid-air image and transmitted light, if any, from the total as described above. If the value obtained is greater than zero, then stray light is judged to be present.

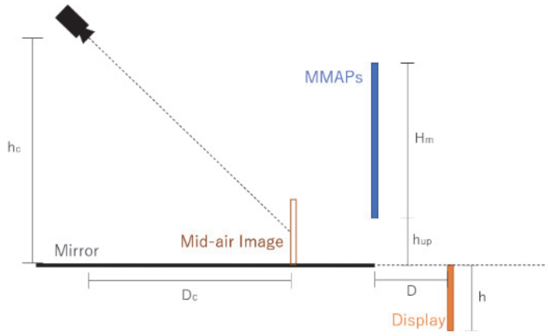

Fig. 4 Optics Structure of EnchanTable

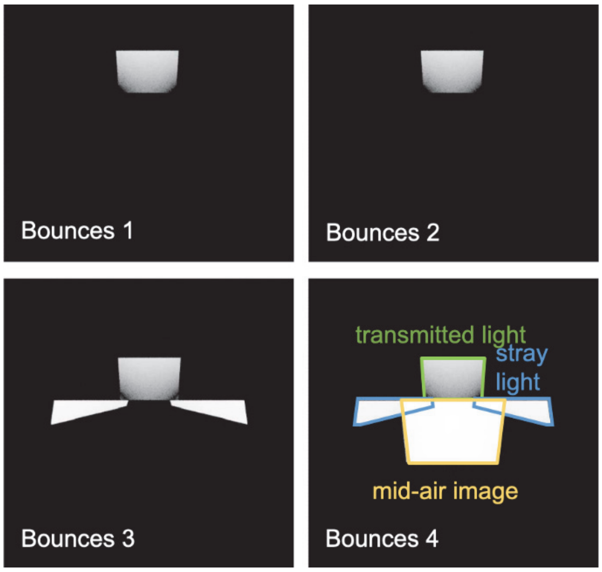

Fig. 5 Rendering results for different numbers of bounces

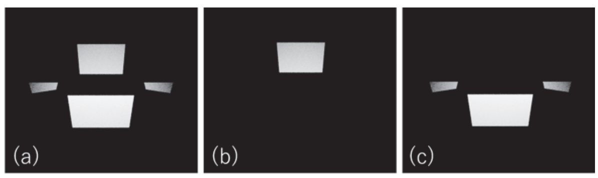

Fig. 6 (a) a mirror is used to display the mid-air image (b) an absorber sheet is used (c) difference between (a) and (b)

For each number of bounces, the transmitted light is removed by rendering the display surface of the mid-air image in two ways, as a mirror and as a light-absorbing surface, and taking the difference. In this design, the mid-air image and stray light can be observed only when the display surface is made of a material that can reflect light, such as a mirror, as shown in Fig. 6. Because the transmitted light reaches the back of the display surface, it can be observed regardless of the display surface material. This is used to remove transmitted light, as shown in Fig. 6 (c), by subtracting the rendered image with a light-absorbing surface from the rendered image with a mirror.

The results of the simulation were compared with those of the actual optics. As shown in Fig. 7, the positions of the mid-air image, stray light, and transmitted light were almost the same as in reality.

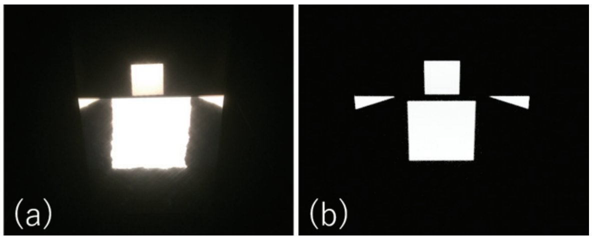

Fig. 7 Comparison of actual (a) and simulated (b) images

6 Reproducibility check for related work

To date, various types of retroreflective transmission optics have been proposed. Depending on the optics application type, reflection, refraction, and diffusion, which occur in devices other than MMAPs, are commonly used. One example that uses refraction is InFloasion [11]. In this optical system, in order to display an undistorted image inside the transparent object, the distortion of the image is compensated for by placing a second transparent object of the same shape as the target transparent object on the light source side. As an example of using reflections, the optical system of Matsumura et al. [12] solves the depth-reversal problem that occurs in MMAPs optics by using multiple reflections in mirrors. An example that uses diffusion is the Shadowless Projector [13]. This is a projection optical system that implements an unshielded projection system by re-projecting the image, which is projected onto a diffused object, onto an object placed at a face-symmetrical position using MMAPs.

The MMAPs can be combined with a variety of optical elements to achieve various video implementations that are not limited to mid-air images. However, as the number of elements in the optical system increases, the design parameters, such as light source size, image formation position, stray light, viewing area, and so on, must be considered in order to find the optimal image display. To realize these complex optical designs without building the optical system, a simulator is required.

Fig. 8 shows the results of our simulation, and Fig. 9 demonstrates the setup for rendering. As a result, it was able to reproduce the characteristics of the optical system and its image formation, including reflective and refractive materials. However, it was found that an optical system containing diffused material could reproduce the properties of the optical system; however, the image was not projected correctly onto the diffused object. The details of the experiment are described in [10].

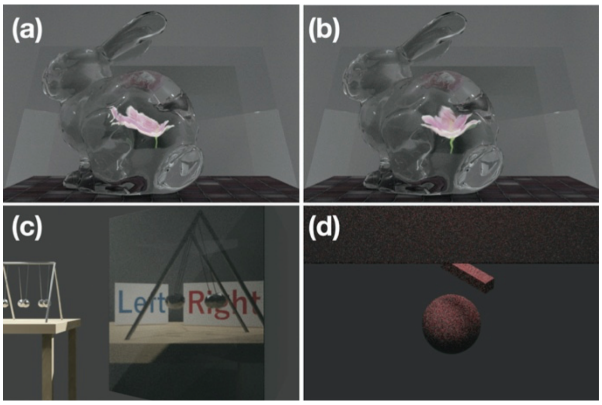

Fig. 8 Simulated optical system. (a) uncompensated InFloasion, (b) compensated InFloasion, (c) depth-reversal resolution using reflections, and (d) Shadowless Projector

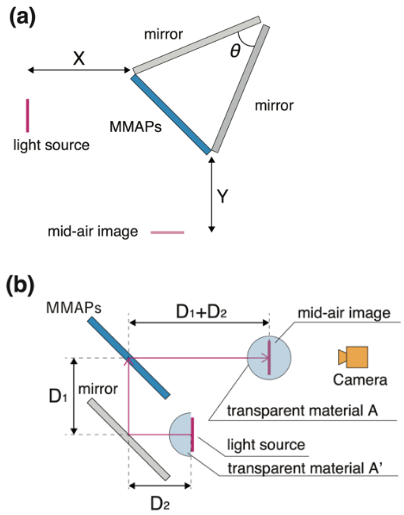

Fig. 9 (a) Schematic diagram of the optical system to eliminate depth inversion of mid-air images by Matsumura et al. (b) Schematic diagram of the optical system of InFloasion

The diffusion was simulated using an optical system for the Shadowless Projector [12], which resolves the shielding of projected images by real objects through MMAPs. In this optical system, an unobstructed projection optical system is realized by using MMAPs to transfer the image, which is projected onto the target object mirror image, to a target object placed at a face-symmetrical position. A schematic diagram of the system is shown in Figure 10(a), where MMAPs are modeled at 48.8 cm on one side. We set the parameter Roughness+, which expresses the diffuseness of the material, to 1.0

(within the range 0.0–1.0) in order for the material of the object to be projected as an ideal, perfectly diffused material.

The simulation-rendered optical system is shown in Fig. 10 (b)–(d). As shown in Fig. 10 (c) and (d), the shadow caused by the shielding object is reduced. However, the image that should be projected is a checkered pattern, as shown in Fig. 10 (d), whereas in Fig. 10 (c), no checkered pattern is observed, and only a light red image is projected. From this, we can state that it is difficult to project the image onto a diffuse object in this simulation environment. This may be a result of the dependence on Cycles, the rendering engine used in Blender. In the future, we would like to conduct further tests with different rendering engines to confirm the functions required for each.

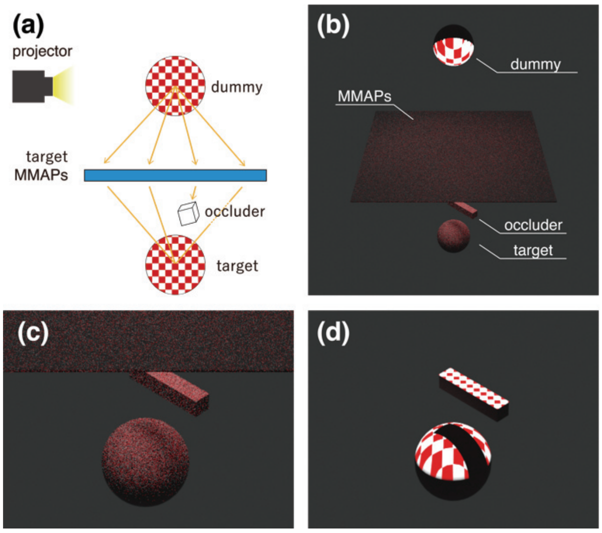

Fig.10 (a) a schematic diagram of the optical system of the Shadowless Projector, (b) the simulation, (c) the projected image, and (d) the image when it is simply projected from above.

7 Conclusion

In this study, we introduced a simulation of MMAPs in Blender. It has been shown that the simulation can reproduce mid-air images and stray light. It was also demonstrated that different combinations of rendering conditions and image processing worked effectively. Moreover, the MMAPs were confirmed to be suitable for application to the simulation of refraction and reflection before and after the MMAPs. However, a limitation exists in combination with diffuse materials. We would like to invite system designers to use MMAPs for real-world applications in the future.

ACKNOWLEDGEMENT

This work was supported by the Canon Foundation.

The author is grateful to Mr. Shunji Kiuchi and Ms. Ayami Hoshi. Mr. Shunji Kiuchi developed a Blender simulation system and re-tested the existing optical system. He primarily led this project. Ms. Ayami Hoshi conducted the computer vision process in our simulation system, and developed automatic stray-light detection. This manuscript is based on their presentations at the 25th *Annual Conference of the Virtual Reality Society of Japan*.

REFERENCES

[1] H. Kakeya, "P-65: FLOATS V: Real-Image-Based Autostereoscopic Display with TFT-LC Filter. SID Symp. Dig. Tech. Pap. 35, pp.490–493 (2004)
[2] T. Huang, X. Zhang, H. Liao, "Floating autostereoscopic display with in situ interaction," *J. Soc. Inf. Disp. 27*, pp. 785–794 (2019)
[3] S. Maekawa, K. Nitta, O. Matoba, "Transmissive optical imaging device with micromirror array," In *Three-Dimensional TV, Video, and Display V*; International Society for Optics and Photonics (SPIE), Vol. 6392, pp. 130–137 (2006)
[4] Y. Yoshimizu, E. Iwase, "Radially arranged dihedral corner reflector array for wide viewing angle of floating image without virtual image. *Opt. Express*, *27*, pp. 918–927 (2019)
[5] M. Otsubo, "Optical Imaging Apparatus and Optical Imaging Method Using the Same," U.S. Patent 8,702.252 B2, (2014)
[6] Y. Maeda, D. Miyazaki, S. Maekawa, "Volumetric aerial three-dimensional display based on heterogeneous imaging and image plane scanning," *Appl. Opt. 54*, pp. 4109–4115 (2015)
[7] H. Yamamoto, Y. Tomiyama, S. Suyama, "Floating aerial LED signage based on aerial imaging by retro-reflection (AIRR)," *Opt. Express*, *22*, pp.26919–26924 (2014)
[8] S, Kiuchi and N. Koizumi, "Micro-mirror array-plates simulation using ray tracing for mid-air imaging," *2020 IEEE Conference on Virtual Reality and 3D User Interfaces Abstracts and Workshops*, pp. 769–770 (2020).
[9] A, Hoshi, S, Kiuchi and N. Koizumi, "Design a mid-air image system without stray light," *The 25th Annual Conference of the VRSJ* 2B3-2, (2020).
[10] S, Kiuchi and N. Koizumi, "Application of Ray Tracing Based Simulation for the Design of Retrotransmission optical system," *The 25th Annual Conference of the VRSJ*, 2B3-2. (2020).
[11] T. Matsumura, S. Sakaguchi, T. Naemura, "Optical System for Eliminating Stereoscopic Depth Reversal of Mid-air Images using a Single Retro-transmissive Plate," IEICE Technical Report, vol. 120, No. 50, MVE2020-2, pp. 5–10, (2020)
[12] T. Yokose, T. Okawa, T. Naemura, "InFloasion: Optical system for displaying images inside transparent objects," IEICE Technical Report, vol. 118, no. 95, MVE2018-6, pp. 89–94, (2018)
[13] K. Hiratani, D. Iwai, P. Punpongsanon and K. Sato, "Shadowless Projector: Suppressing Shadows in Projection Mapping with Micro Mirror Array Plate," *2019 IEEE Conference on Virtual Reality and 3D User Interfaces*, pp. 1309–1310 (2019)